

# A Robust Frequency Controller based on Linear Matrix Inequality for a Parallel Islanded Microgrid

Erum Pathan

Department of Electrical Power Engineering  
Faculty of Electrical and Electronic Engineering  
University Tun Hussein Onn Malaysia  
Johor, Malaysia  
erumasad79@gmail.com

Afarulrazi Abu Bakar

Department of Electrical Power Engineering  
Faculty of Electrical and Electronic Engineering  
University Tun Hussein Onn Malaysia  
Johor, Malaysia  
afarul@uthm.edu.my

Shamsul Aizam Zulkifi

Department of Electrical Power Engineering  
Faculty of Electrical and Electronic Engineering  
University Tun Hussein Onn Malaysia  
Johor, Malaysia  
aizam@uthm.edu.my

Mubashir Hayat Khan

Department of Electrical Power Engineering  
Faculty of Electrical and Electronic Engineering  
University Tun Hussein Onn Malaysia  
Johor, Malaysia  
mubashir.uthm@gmail.com

Haider Arshad

Department of Electrical Power Engineering  
Faculty of Electrical and Electronic Engineering  
University Tun Hussein Onn Malaysia  
Johor, Malaysia  
haiderarshadkhan@gmail.com

Muhammad Asad

Substation Automation Engineer  
NG CSD-C  
Saudi Electricity Company  
Riyadh, Saudi Arabia  
csd\_sec@yahoo.com

**Abstract**-This paper presents a robust  $H^\infty$  control technique for an islanded microgrid in the presence of sudden changes in load conditions. The proposed microgrid scheme consists of a parallel connected inverter with distributed generations. When the load is suddenly changed the frequency deviates from its nominal value. The objective is to design a robust frequency droop controller in order to achieve the frequency at nominal values without using any secondary controller and communication systems while improving power sharing accuracy. Small signal modeling of the power system is designed for the formulation of the problem and the  $H^\infty$  optimal linear matrix inequality technique is applied in order to achieve the objectives. The proposed controller has been tested with the MATLAB/ SimPowerSystem toolbox.

**Keywords**-distributed energy resource; linear matrix inequality (LMI) units; robust control

## I. INTRODUCTION

Conventional power systems change as a consequence of the rising fuel cost and global warming. Distributed Generation (DG) sources are being incorporated to overcome the aforementioned issues. Moreover, modern power systems provide increased reliability and alleviate the pressure on power transmission. A cluster of interconnected DGs is known as a microgrid (MG). The MG has been proposed to integrate DGs to the local loads. Its primary function is to facilitate the

penetration of DGs, and thus enhance the persistence of power supply [1, 2]. The nature of the connected load may be different. It may be of critical or non-critical in nature. However, in any load conditions, the DGs need power converter mechanisms. Consequently, inverters and converters are adapted to connect the DGs to the MG. An MG can be operated in grid-connected or islanded mode to provide reliability and power quality. When a MG is operated in grid-connected mode, at the time of operation the voltage and frequency are fixed by the stiff grid and the DC/AC inverters are connected in parallel to the utility grid, whereas in islanded mode, multiple parallel DGs are required to stabilize voltage and frequency [3]. Voltage and frequency deviation (from nominal values) because of the mismatch between load and generation may lead to complete failure of the MG. So, a robust control strategy is necessary to be taken into account to resolve this control objective in stand-alone operation [4, 5]. A sudden load change will affect the power sharing between two parallel inverters, and the voltage amplitude and frequency will deviate from their nominal values. In order to avoid this problem, a secondary controller has been proposed to restore such deviations. However, the secondary controller fails the concept of distributed power sharing control whereas the communication also needs to be set up. This communication will increase the cost of operation and the complexity of the system while it will reduce reliability and flexibility. Also, such

Corresponding author: Erum Pathan

a system is not easily expanded in remote areas [4, 6]. In order to ensure system's stability and performance, the robust  $H^\infty$  control theory is mostly applied to synthesize a  $H^\infty$  controller by using Linear Matrix Inequality (LMI) technique. It is a robust theoretical powerful tool that can be used directly in finding the optimal solution and therefore reducing the impact of disturbances. The weighted functions are designed properly so they optimally set up the trade-off between robustness and performance in feedback loop. Several methods have been applied in order to resolve the MG frequency control issue [7, 8]. Controlling of frequency deviation has been studied with the help of techniques such as neural networks, fuzzy logic, and Particle Swarm Optimization (PSO) [9]. In the presence of uncertainties, the performance and robustness has also been enhanced by combined PSO-based  $H_2/H^\infty$  [10]. In the traditional techniques the frequency deviation cannot be stabilized in islanded mode when the load is changed. However, the robust control techniques provide effective control synthesis while considering uncertainties and physical constraints [11]. Some researchers have also studied robust control systems for MGs. Distributed robust controllers have been designed for different renewable sources in islanded mode in [12]. A  $\mu$ -synthesis robust controller has been designed through iteration technique in [13]. Other  $\mu$ -synthesis robust controller techniques have been discussed in [14] and the  $H^\infty$  robust controller in [15].

The main contribution of this paper is the proposal of an advanced, control theory-based, robust,  $H^\infty$ , power sharing, non-communication based, controller that restores frequency and improves the accuracy of power sharing, is easy to install, and more reliable without using the secondary existing controller.

II. CONVENTIOANL PRIMARY, EXISTING SECONDARY AND PROPOSED ROBUST  $H^\infty$  POWER SHARING CONTROLLER IN ISLANDED MODE

The first MG layer for control purpose is the primary control, which consists of a combination of the cascaded voltage-current and power sharing controller as given in Figure 1. The cascaded controller is for controlling the inner current controller's signal  $L_i$  and getting the reference signal from the outer voltage controller. The outer voltage controller's signal is from the  $C_f$  of the AC MG system, which can obtain the voltage reference from the frequency signal and the amplitude signal by the power controller. The grid-side inverter current and voltage of the filter capacitor are determined to calculate the average power supplied by each distributed power inverter. The power sharing controller can be implemented for calculating the reference voltage and frequency. Hence, the power sharing controller uses the non-communication power sharing control technique. The power sharing controller comprises of two equations. One of them is the  $P-\omega$  equation, which gives the relationship between the DG active power and the PCC frequency level. In power sharing technique, frequency deviations occur when the MG is operated in islanded mode since frequency is dependent on the connected load. Therefore, a secondary control layer is used to compensate the frequency deviation issue of the power sharing strategy.

The secondary controller transfers the signal of frequency  $\omega_{sec}$ , which adds offsets to the primary controller through the communication links, as illustrated in Figure 1. A synchronous reference frame phase lock loop is implemented to the secondary controller. The basic concept is that the frequency of the output voltage is a global variable in the MG, hence, by controlling the reference angle which extracts the frequency from the PCC, the signal is fed back and compared to the reference signal  $\omega^*$  to generate the error which must be reset by the secondary controller. The delay block is modelled with a 10ms low-pass filter. The point of common coupling voltage and frequency are regulated by the secondary control layer. The proposed  $H^\infty$  controller is shown with the blue-dashed area in Figure 1, where the robust power sharing controller considers the MG frequency and active power. There are two primary problem formulations in this study, which are:

- The frequency deviation when the load is suddenly changed, without applying a hierarchical secondary-level communication-based controller.
- The accuracy of active power sharing according to DG's rating.

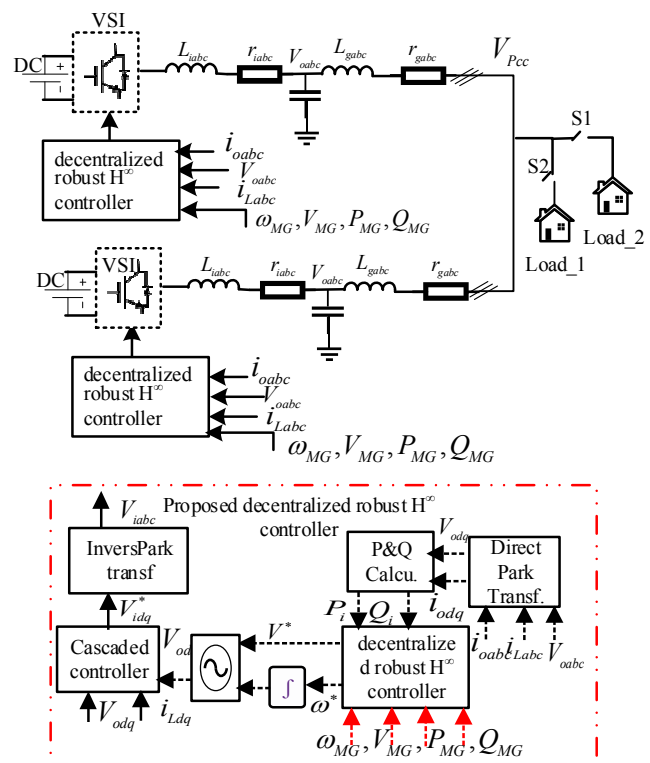


Fig. 1. Block diagram of the conventional primary controller, existing hierarchical secondary controller, and proposed robust  $H^\infty$  decentralized power sharing controller.

III. PROPOSED CONTROLLER VIA LMI OPTIMISATION

The standard robust  $H^\infty$  power sharing controller is configured to achieve the accuracy of power sharing and no frequency deviation. A systematic design procedure is adopted for designing the controller. Open-loop block diagram can be

formulated into a standard configuration by using Linear Fractional Transformation (LFT) [15, 16] and building an augmented system model. The complete virtual augmented system model with exogenous input, output, sensed signal, and control signal is illustrated in Figure 2, where  $G(s)$  is the nominal plant,  $u$  is the input of the system control vector and  $v$  is the sensed output of the controller that needs to be minimized.  $\omega=[\omega_o \ \omega_{MG} \ P_{MG}]^T$  represents a vector of exogenous inputs such as reference signals and disturbances. The external disturbances are unknown, thus they need to be minimized in order to improve the performance specification of the system.  $\Delta z=[z_1 \ z_2]^T$  represents the regulated output signals and the  $[W_1 \ W_2]$  weighted functions are used to shape the control input and achieve good tracking performance.  $K$  is the conventional power sharing controller. The goal is to minimize the  $H^\infty$  norm of the transfer function  $\Delta\omega \rightarrow \Delta z$  and replace the conventional power sharing controller with a robust  $H^\infty$  controller. The main function of the implemented robust  $H^\infty$  controller is to collect the information from  $\Delta v$  and generate the control signal  $\Delta u$ , which antagonizes the influence of  $\Delta\omega \rightarrow \Delta z$ , which in turn minimizes the norm from  $\Delta\omega \rightarrow \Delta z$ .

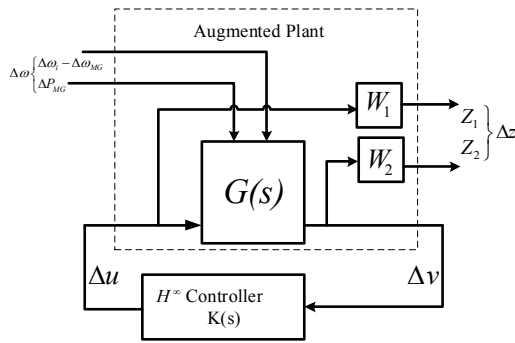


Fig. 2. Augmented plant.

The  $H^\infty$  controller is  $H^\infty(s)=[K(s)]$ . The linear fractional representation of the overall system is represented in (1):

$$\begin{bmatrix} Z_1 \\ Z_2 \\ \dots \\ v \end{bmatrix} = \begin{bmatrix} 0 & 0 & 0 & \dots & W_1 I \\ W_2 G & -W_2 G & 0 & \dots & W_2 G \\ \dots & \dots & \dots & \dots & \dots \\ -HG & HG & I & \dots & HG \end{bmatrix} \begin{bmatrix} \omega_o \\ \omega_{MG} \\ P_{MG} \\ \dots \\ u \end{bmatrix} \quad (1)$$

The control object of  $P$  is augmented by the nominal plant with the norm of weighted functions  $W_1, W_2$  via applying MATLAB's hinfsyn and mixsyn algorithms. The robust power sharing controller is based on a lower bandwidth than the inner cascaded controller. Therefore, a low-pass Butterworth filter at 20Hz is chosen for  $W_2$  to minimize the sensitivity of frequency, and the control effort can be assured to be within the saturation limits. A weighted function  $W_1$ , which is the integral gain constant with the diagonal matrix, is chosen. The diagonal values of the matrix are the inverse of the active power DC gain, which adjusts the power set-point of the voltage source inverters in order to minimize the sensitivity of the active power. The input sensitivity is  $W_2=(0.09 \cdot F)$ , where  $F$  is the

second-order discrete Butterworth low-pass filter with a cut-off frequency of 20Hz. If the range of the frequency is different, the sensitivity and the complementary sensitivity cannot meet the  $H^\infty$  constraint and system's response will not be properly stable. The reduced design of the  $H^\infty$  controller is given as:

$$K(s) = \frac{0.0001783 s^3 + 0.1508 s^2 + 59.56 s + 9938}{s^4 + 4.537e05 s^3 + 1.029e11 s^2 + 1.168e16 s + 4.029e18} \quad (2)$$

The closed-loop transfer function is represented (3) by LFT:

$$T_{oz} = P_{11}(s) + P_{12}(s)K(s)[I - P_{22}(s)K(s)]^{-1}P_{21}(s) \quad (3)$$

The controller  $K(s)$  can be chosen by applying  $H^\infty$  optimal control problems. The main purpose of designing the robust  $H^\infty$  controller is to minimize the  $H^\infty$  norm, which is represented as  $\|T_{oz}\|^\infty < 1$ . Equation (2) is developed in MATLAB environment and normhinf was used to calculate the stability of the closed-loop system. The resulting  $\|T_{oz}\|^\infty$  is 0.654, which ensures that the closed-loop system is stable.

#### IV. SIMULATION AND DISCUSSION

A model with two parallel DG-based MGs in islanded mode is built in MATLAB/Simulink (Figure 3). During the switching from low to medium loads (resistive), time domain response of current and voltage at the point of common coupling, power sharing of MG, voltage, and frequency are analyzed in order to check the effectiveness of the proposed robust  $H^\infty$  power sharing controller over the secondary hierarchical controller and the conventional decentralized primary power sharing controller. In Table I the parameters of the parallel inverter AC MG and the controller can be seen along with the load ratings and switch On-Off times.

TABLE I. PARALLEL INVERTER AC MG, CONTROLLER PARAMETERS AND LOAD RATINGS WITH SWITCH ON-OFF TIMES

Parameters	Values	Parameters	Values
$r_i=r_g$	100mΩ	$m=n$	0.0001
$L_i=L_g$	1.5mH	$k_{pc}$	5.29
$C_f$	25μF	$k_{pv}, k_{iv}$	0.041, 35
$\tau_{pll}$	10ms	$k_{psec}$	0.150
$P_{L1}$	365W (0-1 s)	$k_{i_{sec}}$	9k <sub>psec</sub>
$P_{L2}$	730W (1-2 s)	$\omega$	31.415rad/s
$V_{dc}$	700V	$\omega_c$	2pi10rad/sec

##### A. Time Domain Analysis of Voltage/Current at the Point of Common Coupling

The voltage and current analysis at the Point of Common Coupling (PCC) are given in this section. Figures 4 and 5 present the voltage and current responses at the PCC level of the proposed robust  $H^\infty$  controller, the conventional and the secondary controller-based systems along with the zoomed pictures for clear visualisation. The load current is contributed by the parallel islanded DGs when two different loads are connected. At time 0-1s and using load 365W, the consumed current is nearly 0.73A and the voltage peak is around 311.12V. When the load is slightly changed at 1s, the proper sinusoidal signal continues again. In addition, when a load of 730W is connected at 1-2s, the consumed current is

approximately 1.457A for the secondary and the proposed robust  $H^\infty$ -based parallel DGs. When the conventional system is observed, there is a slight difference in current and voltage at the PCC. At 0-1s, the current and voltage are approximately 0.699A and 311V respectively, and during the second load at 1-2s, the current and voltage are around 1.4A and 310.2V

respectively. There is a spike in the current and the voltage slightly changes, however it is still stable. This shows that smooth transient voltage and current are flowing when the load is suddenly changed, and the parallel islanded system's behavior is stable.

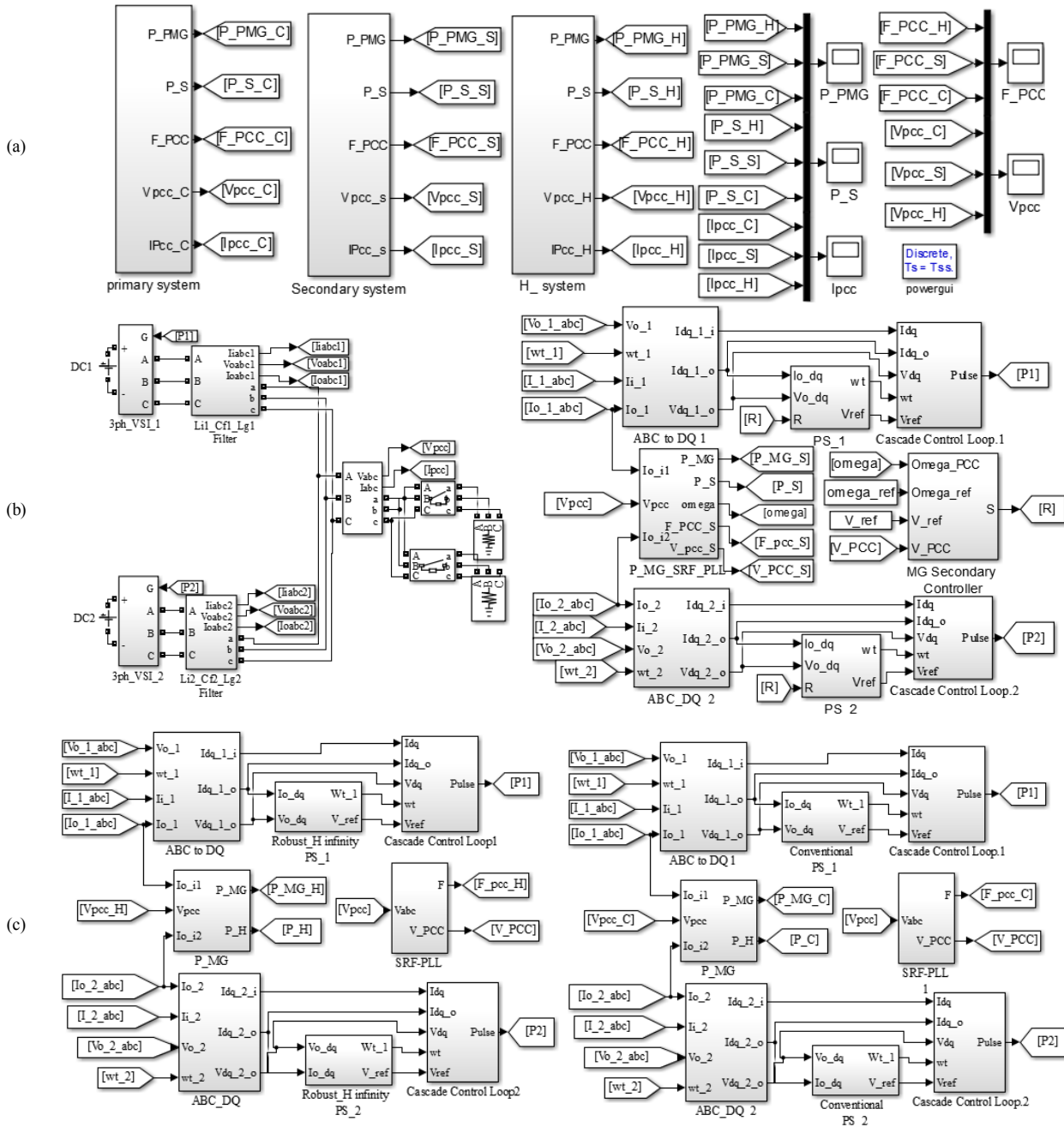


Fig. 3. Comparison: (a) Simulation model, (b) electrical system and existing secondary, (c) conventional and proposed robust  $H^\infty$ .

**B. Time Domain Analysis of DGs' Sharing Power and Microgrid Power**

At a second stage, the analysis takes into account the

transient behavior of active power sharing of  $DG_1$  and  $DG_2$  as well as the total MG average power, which are illustrated in Figure 6 and Figure 7 respectively.

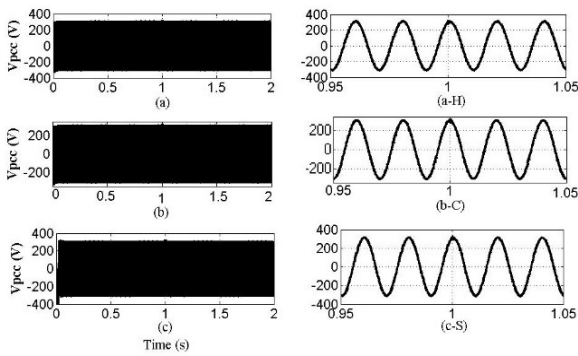


Fig. 4. Voltage response at PCC: (a)  $H^\infty$  voltage at PCC and (a-H) zoomed picture, (b) conventional voltage at PCC and (b-C) zoomed picture, (c) secondary voltage at PCC, and (c-S) zoomed picture.

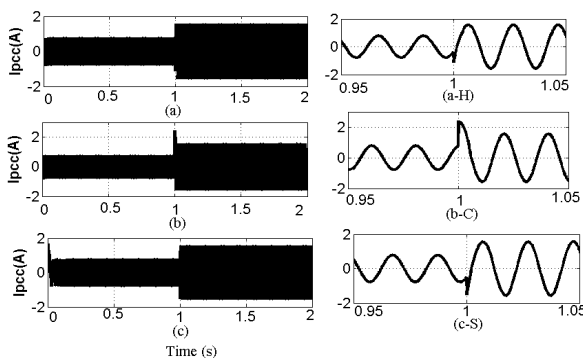


Fig. 5. Current response at PCC: (a)  $H^\infty$  current at PCC and (a-H) zoomed picture, (b) conventional current at PCC and (b-C) zoomed picture, (c) secondary current at PCC (c), and (c-S) zoomed picture.

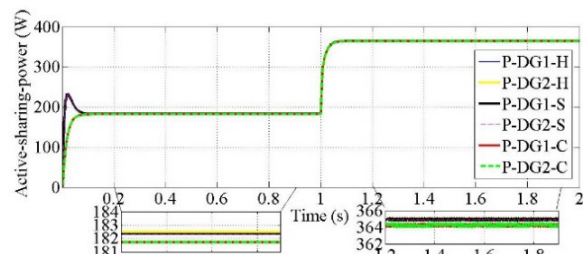


Fig. 6. Active sharing power time domain response (H=robust  $H^\infty$  control, S=secondary hierarchical control, C=conventional primary hierarchical control).

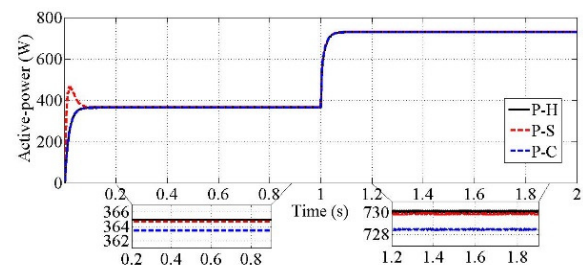


Fig. 7. Active power time domain response (H=robust  $H^\infty$  control, S=secondary hierarchical control, C=conventional primary hierarchical control)

The proposed controller, the hierarchical primary controller, and the secondary controller change condition under

low-to-medium sudden load. The simulation time is 0-1s when a low load of 365W is connected. Each DG's active sharing power is approximately 181.8W in the hierarchical primary conventional controller. Meanwhile, the proposed robust  $H^\infty$  controller and the hierarchical secondary control loop share the active power in each DG at about 182.489W. Additionally, when the second medium load of 730W is connected at 1-2s the sharing of each DG's active power is approximately 364.245W using the conventional hierarchical primary controller. On the other hand, the secondary hierarchical controller and the robust  $H^\infty$  controller are sharing power at around 365W during low-to-medium load sharing. It can be noticed that the sharing of active power has been improved without using any communication technique in the proposed robust  $H^\infty$  controller and in the hierarchical secondary controller, though the hierarchical secondary controller has failed the concept of plug-and-play because it requires communication. While the conventional hierarchical primary controller has no communication, the sharing of power is not equal to the ratings of the DGs. Figure 7 depicts the active MG power of around 363.6W when using the conventional hierarchical primary controller. When the proposed robust  $H^\infty$  controller is applied, the power is approximately 365W and is similar to the secondary hierarchical controller at low load. When the load is suddenly switched from low to medium, the MG power using a conventional controller is approximately 728.5W at 1-2s while the proposed robust  $H^\infty$  controller and the secondary hierarchical communication-based controller have almost similar active MG power of around 730W.

C. Time Domain Analysis of Frequency Restoration

This section analyzes the effectiveness of the proposed robust  $H^\infty$  controller in terms of frequency restoration during sudden low-to-medium load changes. In addition, signals from the secondary communication-based hierarchical controller and the conventional primary decentralized non-communication-based hierarchical controller are compared with the proposed controllers (Figure 8(a)).

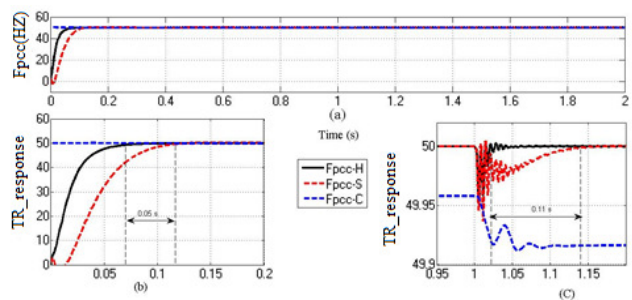


Fig. 8. (a) Frequency time domain response, (b) transient frequency response at PCC, and (c) transient response of sudden load change.

Figure 8(b) indicates the step response of the conventional, the existing secondary, and the proposed controller. The response under the existing secondary controller frequency is slower by 0.12s in rise time because of processing delay, whereas the proposed robust  $H^\infty$  controller is demonstrated in fast manner with 0.06s and reaches steady state faster than the existing secondary controller. Figure 8(c) indicates that the

frequency deviates more with sudden load using the conventional primary hierarchical controller at around 49.92Hz. Transient is also slower than the proposed controller at step time 1-2s. On the other hand, the secondary controller shows a slower rise time of 1.145s with high peak at 1.01s with 40% overshoot and slower steady state level because of processing delay. The proposed robust  $H^\infty$  controller restores the frequency and retains the nominal frequency during a sudden load change in a faster manner with 1.02s rise time. From the Figure, it is clear that the proposed controller's overshoot is reduced to 6%. The controller efficiency response increased by 95% for reference value tracking. Moreover, it has the capability to restore the frequency response faster to nominal value than the conventional and the existing secondary controller. Consequently, the proposed robust  $H^\infty$  controller and the secondary hierarchical loop restore frequency within the specified range given in the respective IEEE standard [17].

## V. CONCLUSION

A systematic designing procedure of robust frequency droop controllers has been presented. The proposed MG consists of parallel connected DC sources with loads which are suddenly changed and the controller shows its robustness to maintain the frequency at its nominal value in very short time in comparison with the secondary hierarchical controller and the conventional controller without using any communication links. All the effective signals are considered here as disturbances and the proper weighted function and proper  $H^\infty$  controller were designed for achieving the desired objective by using LMI technique. The proposed controller was simulated in MATLAB and the results were compared with the results of the conventional and the secondary controllers.

## REFERENCES

- [1] R. H. Lasseter, "MicroGrids," in *2002 IEEE Power Engineering Society Winter Meeting. Conference Proceedings (Cat. No.02CH37309)*, Jan. 2002, vol. 1, pp. 305–308 vol.1, doi: 10.1109/PESW.2002.985003.
- [2] N. Bayati, S. H. H. Sadeghi, and A. Hosseini, "Optimal Placement and Sizing of Fault Current Limiters in Distributed Generation Systems Using a Hybrid Genetic Algorithm," *Engineering, Technology & Applied Science Research*, vol. 7, no. 1, pp. 1329–1333, Feb. 2017.
- [3] M. Illindala and U. Venkataramanan, "Control of distributed generation systems to mitigate load and line imbalances," in *2002 IEEE 33rd Annual IEEE Power Electronics Specialists Conference. Proceedings (Cat. No.02CH37289)*, Jun. 2002, vol. 4, pp. 2013–2018 vol.4, doi: 10.1109/PSEC.2002.1023110.
- [4] E. Pathan, S. A. Zulkifli, U. B. Tayab, and R. Jackson, "Small Signal Modeling of Inverter-based Grid-Connected Microgrid to Determine the Zero-Pole Drift Control with Dynamic Power Sharing Controller," *Engineering, Technology & Applied Science Research*, vol. 9, no. 1, pp. 3790–3795, Feb. 2019.
- [5] Q. L. Lam, A. I. Bratcu, D. Riu, C. Boudinet, A. Labonne, and M. Thomas, "Primary frequency  $H^\infty$  control in stand-alone microgrids with storage units: A robustness analysis confirmed by real-time experiments," *International Journal of Electrical Power & Energy Systems*, vol. 115, p. 105507, Feb. 2020, doi: 10.1016/j.ijepes.2019.105507.
- [6] J. M. Guerrero, J. Matas, L. Garcia de Vicuna, M. Castilla, and J. Miret, "Decentralized Control for Parallel Operation of Distributed Generation Inverters Using Resistive Output Impedance," *IEEE Transactions on Industrial Electronics*, vol. 54, no. 2, pp. 994–1004, Apr. 2007, doi: 10.1109/TIE.2007.892621.
- [7] I. Șerban and C. Marinescu, "Aggregate load-frequency control of a wind-hydro autonomous microgrid," *Renewable Energy*, vol. 36, no. 12, pp. 3345–3354, Dec. 2011, doi: 10.1016/j.renene.2011.05.012.
- [8] W. Gu, W. Liu, Z. Wu, B. Zhao, and W. Chen, "Cooperative Control to Enhance the Frequency Stability of Islanded Microgrids with DFIG-SMES," *Energies*, vol. 6, no. 8, pp. 1–21, 2013.
- [9] H. Bevrani, F. Habibi, P. Babahajyani, M. Watanabe, and Y. Mitani, "Intelligent Frequency Control in an AC Microgrid: Online PSO-Based Fuzzy Tuning Approach," *IEEE Transactions on Smart Grid*, vol. 3, no. 4, pp. 1935–1944, Dec. 2012, doi: 10.1109/TSG.2012.2196806.
- [10] X. Li, Y.-J. Song, and S.-B. Han, "Frequency control in micro-grid power system combined with electrolyzer system and fuzzy PI controller," *Journal of Power Sources*, vol. 180, no. 1, pp. 468–475, May 2008, doi: 10.1016/j.jpowsour.2008.01.092.
- [11] Q. L. Lam, A. I. Bratcu, and D. Riu, "Frequency robust control in stand-alone microgrids with PV sources: design and sensitivity analysis," in *Symposium de Génie Electrique*, Grenoble, France, Jun. 2016.
- [12] A. H. Etemadi, E. J. Davison, and R. Iravani, "A Decentralized Robust Control Strategy for Multi-DER Microgrids—Part I: Fundamental Concepts," *IEEE Transactions on Power Delivery*, vol. 27, no. 4, pp. 1843–1853, Oct. 2012, doi: 10.1109/TPWRD.2012.2202920.
- [13] Y. Han, P. M. Young, A. Jain, and D. Zimmerle, "Robust Control for Microgrid Frequency Deviation Reduction With Attached Storage System," *IEEE Transactions on Smart Grid*, vol. 6, no. 2, pp. 557–565, Mar. 2015, doi: 10.1109/TSG.2014.2320984.
- [14] A. Kahrobaei and Y. A.-R. I. Mohamed, "Direct Single-Loop /spl mu-/Synthesis Voltage Control for Suppression of Multiple Resonances in Microgrids with Power-Factor Correction Capacitors," *IEEE Transactions on Smart Grid*, vol. 4, no. 2, pp. 1151–1161, Jun. 2013, doi: 10.1109/TSG.2012.2228014.
- [15] M. Babazadeh and H. Karimi, "A Robust Two-Degree-of-Freedom Control Strategy for an Islanded Microgrid," *IEEE Transactions on Power Delivery*, vol. 28, no. 3, pp. 1339–1347, Jul. 2013, doi: 10.1109/TPWRD.2013.2254138.
- [16] S. Skogestad and I. Postlethwaite, *Multivariable Feedback Control: Analysis and Design*, 2nd Edition. Chichester: Wiley-Interscience, 2005.
- [17] 2030.7-2017 - IEEE Standard for the Specification of Microgrid Controllers. IEEE, 2018.